

## Annealing Effect on the Microstructure and Mechanical Properties of a Thin Titanium Nitride Film

S. C. Her<sup>1</sup> and C. L. Wu

Department of Mechanical Engineering, Yuan Ze University, Chung-Li, Taiwan

<sup>1</sup> mesch@saturn.yzu.edu.tw

УДК 539.4

## Влияние отжига на микроструктуру и механические свойства тонкой нитрид-титановой пленки

Ш. Ч. Хер<sup>1</sup>, Ч. Л. Ву

Факультет машиностроения, Университет Юань Зе, Чунг-Ли, Тайвань

*Методом магнетронного напыления при постоянном токе на стальную подложку SUS 304 наносили нитрид-титановые пленки. Детально исследовано влияние отжига после нанесения пленок на микроструктуру и их механические свойства с помощью метода атомно-силовой микроскопии, стабилизатора напряжения и наноиндентирования. Нитрид-титановые пленки обжигали при температуре 100...300°C. Шероховатость их поверхности, исследуемая методом атомно-силовой микроскопии, уменьшилась с 3,83 до 2,43 нм при повышении температуры отжига в интервале 100...300°C. Скорость коррозии пленок, измеренная с помощью стабилизатора напряжений в 0,5%-ном молярном растворе H<sub>2</sub>SO<sub>4</sub>, снизилась с  $8,57 \cdot 10^{-2}$  до  $4,59 \cdot 10^{-2}$  мм, тогда как температура отжига повысилась с 100 до 300°C. Рост коррозионной стойкости зависит от увеличения твердости и модуля упругости пленки с температурой отжига. Исследование пленки посредством метода атомно-силовой микроскопии показало, что нитрид титана, который обжигался при более высокой температуре, имеет мелкозернистую структуру. Установлено, что механические свойства нитрид-титановых пленок можно значительно улучшить путем отжига. Получил подтверждение тот факт, что контроль процесса отжига крайне необходим для усовершенствования свойств нитрид-титановых пленок.*

**Ключевые слова:** магнетронное напыление, нитрид-титановые пленки, отжиг, наноиндентирование.

**Introduction.** In recent years, titanium nitride (TiN) films have been widely used for many industrial applications, e.g., for improvement of corrosion resistance and wear protection of cutting tools [1] and machine components [2], because TiN possesses high hardness, thermal stability, low friction coefficient, corrosion and erosion resistance [3]. TiN with sufficient biocompatibility is also considered as an important biomaterial [4–7]. Hadad et al. [8] reported that the addition of up to 30% of titanium nitride to silicon nitride matrix led to an improvement of wear resistance of migration of metal atoms from the interconnects into adjacent dielectric [9]. TiN is one of the most widely used diffusion barrier materials [10]. TiN films grown by physical vapor deposition (PVD) on a substrate, will inevitably have residual stress after the process is complete. The residual stress is also a significant factor on influencing preferred orientation, adhesion, and hardness of the film [11]. An excessive stress can lead to cracking of the film in the case of tensile stress and to buckling in the case of compressive stress. Machunze and Janssen [12] deposited TiN films

on silicon substrate using unbalanced magnetron sputter. They found that the average film stress is highly compressive in thin films and less compressive in thicker ones. Lee et al. [13] investigated the effect of TiN coating on electrochemical behavior of Ti alloys. The wear resistance of TiN is often attributed to the high hardness as well as to good chemical stability. The achievement of high hardness and high toughness ought to be linked to the large number of internal interfaces, which act as sites of energy dissipation and crack deflection. Carvalho and De Hosson [14] described the results of an investigation to determine the relationship between microstructure, deformation mechanisms, and mechanical properties of TiN/(Ti,Al)N multilayers subjected to nanoindentation. Wittling et al. [15] investigated the influence of coating thickness and substrate type on the hardness and deformation of TiN films on high-speed steel, silicon and sapphire substrates through nanoindentation with a Berkovich indenter. Sun and co-workers [16, 17] used the finite element analysis to investigate the plastic behavior of various TiN coating/substrate systems for a range of different substrates with different properties. Ma et al. [18] studied the deformation mechanisms of a range of TiN coatings with different thicknesses deposited on the V820 steel substrate. The performance of tribological coatings depends greatly on the adhesion strength between the coatings and substrates. Liu et al. [19] investigated the influence of the ion implantation energy of nitrogen on the adhesion and surface properties of TiN deposited on aluminum substrate.

Magnetron sputtering provides a wide variation of the deposition parameters which affect the microstructure and morphology of the films and, consequently, their properties. In this work, TiN thin films were deposited by D.C. magnetron sputtering process on the SUS 304 steel substrate. The effects of annealing temperature on the morphology and mechanical properties of the TiN films were investigated. The microstructure and surface roughness of the TiN films were examined using atomic force microscopy. The elastic modulus and hardness are the key parameters in the study of wear and adhesion of thin films to the substrates and their responses to the mechanical loads. Since the mechanical properties of the nanomaterials may be significantly different from those of bulk materials, there is a need to study the mechanical properties of the thin film at the nanoscale. Various techniques have been developed for evaluating the mechanical properties of thin films. Among them, nano-indentation [20, 21] has become the most widely adopted technique in the study of the mechanical properties, such as hardness and elastic modulus, on small scale or near surfaces. In this study, nanoindentation tests were employed to determine hardness and the elastic moduli of TiN films with different annealing temperatures. The effects of annealing temperature on the corrosion behavior were investigated using the electrochemical method.

**Film Preparation.** A series of TiN films were prepared by D.C. magnetron sputtering system (ULVAC MB06-4703) on the SUS 304 steel substrate. The target was a titanium disk (2 inch diameter) with a purity of 99.995%. The distance between the target and substrate was approximately 15 cm. The target was sputtered in high-purity argon (99.999%) and nitrogen (99.999%) plasma. Prior to deposition, the substrates were cleaned in soap solution, submerged into acetone and ethanol solutions and in an ultrasound bath for 10 min after rinsing with distilled water. Then the substrates were dried in an oven at the temperature of 50°C for 30 min before the application of deposition. The chamber was equipped with a rotary vane pump and a turbo pump. After the pumping period of two hours, the chamber was evacuated down to a base pressure of  $8 \cdot 10^{-4}$  Pa. Before the application of deposition, the Ti target and substrate were sputter-cleaned to remove the oxide and contaminant. TiN films were deposited at the operation pressure of about  $6 \cdot 10^{-1}$  Pa with the duration of 80 min for all the prepared samples. The as-prepared films were post-annealed at different temperatures in air to investigate the effect of annealing temperature on the microstructure and mechanical properties. The annealing was performed at temperatures of 100, 200, and 300°C for 80 min. Then, the samples were allowed to cool

down to the room temperature in their environment. The thicknesses of TiN films were measured by the surface profiler (KLA Tencor P16). To obtain the film thickness, a small tape was placed at the substrate prior to deposition to get a step on the sample surface. The step height was measured in different points on the sample surface, and the film thickness was taken as the average of these values. The thicknesses of TiN films annealed at different temperatures of 100, 200, and 300°C, are 195, 181, and 174 nm, respectively. One can see that the film thickness decreases with the increase of annealing temperature.

**Microstructure and Surface Topography.** The microstructure and surface topography of TiN films were examined using atomic force microscopy (Seiko Instruments Inc. SPA 400). The AFM was operated in the tapping mode. The AFM images depicted in Fig. 1 show that the films annealed at high temperature of 200 and 300°C have relatively smooth surface and compact structure. The surface roughness decreased with the increase of the annealing temperature as shown in Table 1. More energy was supplied to the molecules at higher temperatures resulting in the higher migration mobility, which in turn favored the formulation of a smoother and denser film. This observation was in agreement with the surface roughness and film thickness listed in Table 1.

T a b l e 1

**Surface Roughness and Thickness of TiN Film with Various Annealing Temperatures**

Annealing temperature (°C)	100	200	300
Surface roughness RMS (nm)	3.83	2.94	2.43
Film thickness (nm)	195	181	174

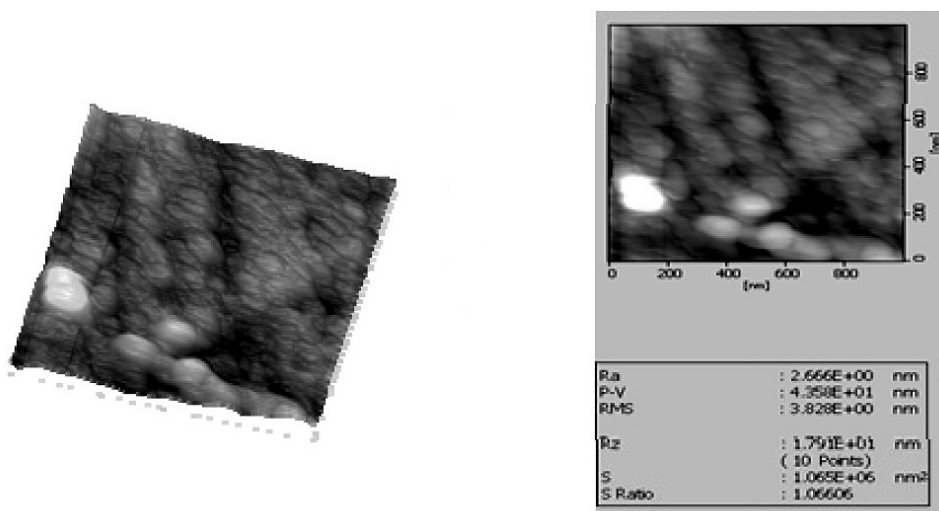


Fig. 1. AFM images of TiN films with annealing temperature 100°C.

**Nanoindentation Test.** The mechanical properties (hardness and elastic modulus) of TiN films were characterized using nanoindentation techniques. Oliver and Pharr [20, 21] developed the most comprehensive method for determining the hardness and modulus from load–indentation curve. The results were analyzed according to the equation

$$S = 2aE_r = \frac{2\beta}{\sqrt{\pi}} E_r \sqrt{A}, \quad (1)$$

where  $a$  is the contact radius and  $A$  is the projected contact area, whereas  $\beta$  is used to account for the geometric shape of different indenters. For a Berkovich indenter  $\beta = 1.034$ . Here  $S$  is the contact stiffness corresponding to the slope of the load–indentation curve at the beginning of the unloading.  $E_r$  is the reduced modulus expressed in terms of the elastic modulus  $E$  and Poisson’s ratio  $\nu$  of the indenter and the indented material as follows:

$$\frac{1}{E_r} = \frac{1-\nu_s^2}{E_s} + \frac{1-\nu_i^2}{E_i}, \tag{2}$$

where subscripts  $i$  and  $s$  represent the indenter and substrate, respectively. For a diamond Berkovich indenter  $E_i = 1140$  GPa and  $\nu_i = 0.07$ .

The hardness was determined using the equation

$$H = \frac{P_{\max}}{A_c}, \tag{3}$$

where  $A_c$  is the area of the indentation at the maximum applied load  $P_{\max}$ . By knowing precisely the geometry of the indenter,  $A_c$  can be expressed in terms of the indentation depth  $h$  directly determined from measurements.

In this study, the nanoindentation tests were performed using the Mico Material Co. Nano Test. Indentation was made using a Berkovich indenter calibrated with a standard silica specimen. A typical load–displacement curve consists of three segments: loading to a peak load, holding at the peak and unloading back to the zero load. A holding period of at least 5 s was applied to allow the time-dependent effects to diminish. TiN films annealed at different temperatures were examined by nanoindentation. Figure 2 represents the load–displacement curves of TiN films annealed at 100°C. There are three curves in the figure corresponding to three different indentation depths. By using the continuous stiffness measurement mode, nanoindenter allows the hardness and modulus to be determined as a function of indentation depth.

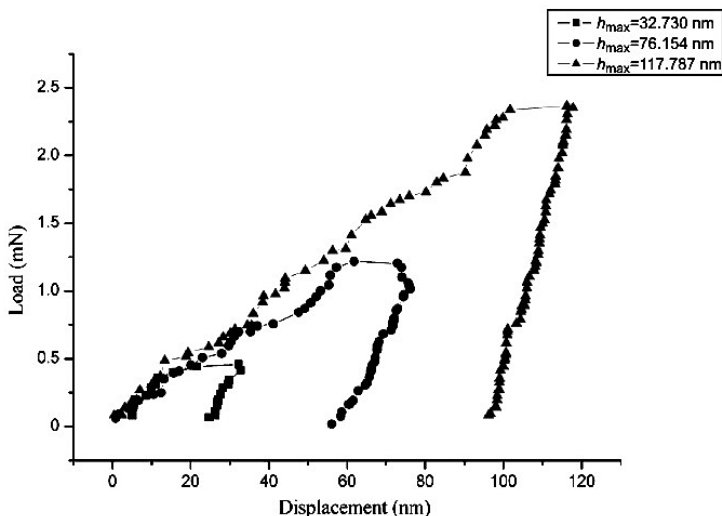


Fig. 2. Load versus displacement of TiN film with annealing temperature 100°C.

The hardness and elastic modulus of TiN films with different annealing temperatures (versus normalized indentation depth) are presented in Figs. 3 and 4, respectively. It can be

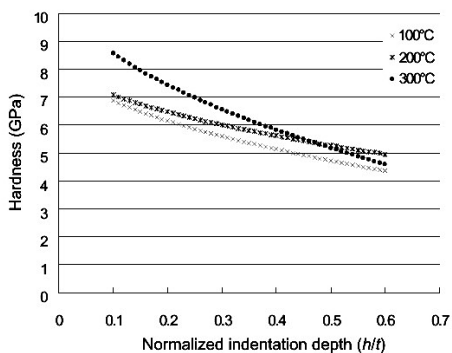


Fig. 3

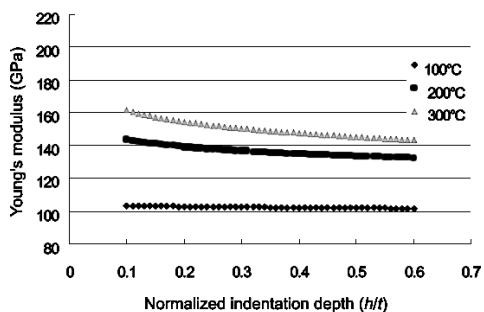


Fig. 4

Fig. 3. Hardness versus indentation depth for TiN films with various annealing temperatures.

Fig. 4. Elastic modulus versus indentation depth for TiN films for various annealing temperatures.

observed that both the hardness and elastic modulus increase with the increase of annealing temperature. This increase is attributed largely to the effects of fine-grained morphology of the film annealed at higher temperature. The measured hardness and elastic modulus values were found to depend on the indentation depth. As shown in Figs. 3 and 4, both hardness and elastic modulus drop with the increase of indentation depth.

**Corrosion Test.** The corrosion behavior of TiN films was investigated using a potentostat (Solartron 1285 potentostat) in 0.5 molar  $H_2SO_4$  solution at room temperature. Electrochemical measurements were carried out with conventional three-electrode configuration consistent with a platinum counter electrode, a saturated calomel reference electrode and a working electrode. The corrosion potential  $\phi_{corr}$  was swept from the initial potential of  $-1\text{ V}$  to the final potential of  $+1\text{ V}$  with a sweep rate of  $10\text{ mV/s}$  for all specimens. The corrosion current density  $J_{corr}$  can be obtained from the polarization curves using the Tafel extrapolation. The corrosion potential, corrosion current density and corrosion rate of TiN films with various annealing temperatures are listed in Table 2. The corrosion rate of TiN film measured by a potentostat in 0.5 molar  $H_2SO_4$  solution decreased from  $8.57 \cdot 10^{-2}$  to  $4.59 \cdot 10^{-2}$  mmPY as the annealing temperature increasing from 100 to  $300^\circ\text{C}$ . The increase in the corrosion resistance is attributed to the increase of hardness and modulus of the film with higher annealing temperature.

Table 2

**Corrosion Potential, Corrosion Current Density, and Corrosion Rate of TiN Film with Various Annealing Temperatures**

Annealing temperature ( $^\circ\text{C}$ )	Corrosion potential (V)	Corrosion current density ( $\text{A}/\text{cm}^2$ )	Corrosion rate (mmPY)
100	$5.17 \cdot 10^{-1}$	$8.27 \cdot 10^{-6}$	$8.57 \cdot 10^{-2}$
200	$4.44 \cdot 10^{-1}$	$7.10 \cdot 10^{-6}$	$7.34 \cdot 10^{-2}$
300	$4.63 \cdot 10^{-1}$	$4.42 \cdot 10^{-6}$	$4.59 \cdot 10^{-2}$

**Conclusions.** The microstructure and mechanical properties of TiN films annealed at different temperatures were investigated in this paper. Experimental results show that annealing temperature plays an important role in modifying the morphology and mechanical properties of TiN films. More energy was supplied to the molecules at higher temperatures

resulting in the higher migration mobility and nucleation density, which in turn favored the formulation of a smoother and denser film. Consequently, surface roughness and film thickness decreased with the increase of annealing temperature. Enhancement in the hardness and elastic modulus of TiN films with the increase of annealing temperature was attributed to the fine grain morphology. The corrosion resistance of TiN films also improved with the annealing temperature increase.

**Acknowledgment.** The authors gratefully acknowledge the financial support provided by National Science Council of R.O.C. under grant No. NSC 101-2622-E-155-015-CC3 for this work.

## Резюме

Методом магнетронного напилення під дією постійного струму на стальну підкладку SUS 304 наносили нітрид-титанові плівки. Детально досліджено вплив відпалу після нанесення плівок на мікроструктуру та їх механічні властивості за допомогою методу атомно-силової мікроскопії, стабілізатора напруги і наноіндентування. Нітрид-титанові плівки випалювали за температури 100...300°C. Шорсткість їхньої поверхні, що досліджувалася методом атомно-силової мікроскопії, зменшилася з 3,83 до 2,43 нм із підвищенням температури відпалу в інтервалі 100...300°C. Швидкість корозії плівок, яку вимірювали за допомогою стабілізатора напруги в 0,5%-ному молярному розчині H<sub>2</sub>SO<sub>4</sub>, зменшилася з  $8,57 \cdot 10^{-2}$  до  $4,59 \cdot 10^{-2}$  мм, у той час як температура відпалу підвищилася із 100 до 300°C. Зростання корозійної стійкості залежить від збільшення твердості і модуля пружності плівки з температурою відпалу. Дослідження плівки за допомогою методу атомно-силової мікроскопії показало, що нітрид титану, який випалювався за більш високої температури, має дрібнозеренну структуру. Установлено, що механічні властивості нітрид-титанових плівок можна значно покращити шляхом відпалу. Отримав підтвердження той факт, що контроль процесу відпалу необхідний для удосконалення властивостей нітрид-титанових плівок.

1. K. Tuffy, G. Byrne, and D. Dowling, "Determination of the optimum TiN coating thickness on WC inserts for machining carbon steels," *J. Mater. Process. Technol.*, **155**, 1861–1866 (2004).
2. Z. D. Cui, S. L. Zhu, H. C. Man, and X. J. Yang, "Microstructure and wear performance of gradient Ti/TiN metal matrix composite coating synthesized using a gas nitriding technology," *Surf. Coat. Technol.*, **190**, 309–313 (2005).
3. M. K. Lee and H. S. Kang, "Characteristics of TiN film deposited on stellite using reactive magnetron sputter ion plating," *J. Mater. Res.*, **12**, No. 9, 2393–2400 (1997).
4. E. Czarnowska, T. Wierzchon, and A. Maran-Niedba, "Properties of the surface layers on titanium alloy and their biocompatibility in vitro tests," *J. Mater. Process. Technol.*, **92**, 190–194 (1999).
5. F. Watari, Y. Tamura, A. Yokoyama, et al., "Mechanical properties and biocompatibility of surface-nitrided titanium for abrasion resistant implant," *Key Eng. Mater.*, **254/256**, 873–876 (2004).
6. J. R. Goldberg and J. L. Gilbert, "In vitro corrosion testing of modular hip tapers," *J. Biomed. Mater. Res. B: Appl. Biomater.*, **64B**, 78–93 (2003).
7. Y. Tamura, A. Yokoyama, F. Watari, and T. Kawasaki, "Surface properties and biocompatibility of nitrided titanium for abrasion resistant implant materials," *Dent. Mater. J.*, **21**, 355–372 (2002).

8. M. Hadad, G. Blugan, J. Kubler, et al., "Tribological behaviour of  $\text{Si}_3\text{N}_4$  and  $\text{Si}_3\text{N}_4$ - $\%$ TiN based composites and multi-layer laminates," *Wear*, **260**, 634–641 (2006).
9. J. W. Elam, M. Schuisky, J. D. Ferguson, and S. M. George, "Surface chemistry and film growth during TiN atomic layer deposition using TDMAT and  $\text{NH}_3$ ," *Thin Solid Films*, **436**, No. 2, 145–156 (2003).
10. A. E. Kaloyeros and E. Eisenbraun, "Ultra thin diffusion barriers/liners for gigascale copper metallization," *Annu. Rev. Mater. Sci.*, **30**, 363–385 (2006).
11. W. J. Chou, G. P. Yu, and J. H. Huang, "Mechanical properties of TiN thin film coatings on 304 stainless steel substrates," *Surf. Coat. Technol.*, **149**, 7–13 (2002).
12. R. Machunze and G. C. A. M. Janssen, "Stress and strain in titanium nitride thin films," *Thin Solid Films*, **517**, 5888–5893 (2009).
13. K. Lee, W. G. Kim, J. Y. Cho, et al., "Effects of TiN film coating on electrochemical behaviors of nanotube formed Ti-xHf alloys," *Trans. Nonferrous Met. Soc. China*, **19**, 857–861 (2009).
14. N. J. M. Carvalho and J. Th. M. De Hosson, "Deformation mechanisms in TiN/(Ti, Al)N multilayers under depth-sensing indentation," *Acta Mater.*, **54**, 1857–1862 (2006).
15. M. Wittling, A. Bendavid, P. J. Martin, and M. V. Swain, "Influence of thickness and substrate on the hardness and deformation of TiN films," *Thin Solid Films*, **270**, 283–288 (1995).
16. Y. Sun, T. Bell, and S. Zhang, "Finite element analysis of the critical ratio of coating thickness to indentation depth for coating property measurements by nanoindentation," *Thin Solid Films*, **258**, 198–204 (1995).
17. Y. Sun, A. Bloyce, and T. Bell, "Finite element analysis of plastic deformation of various TiN coating/substrate systems under normal contact with a rigid sphere," *Thin Solid Films*, **271**, 122–131 (1995).
18. L. W. Ma, J. M. Cairney, M. J. Hoffman, and P. R. Munroe, "Effect of coating thickness on the deformation mechanisms in PVD TiN-coated steel," *Surf. Coat. Technol.*, **204**, 1764–1773 (2010).
19. Y. Liu, L. Li, M. Xu, et al., "Effects of nitrogen ion implantation and implantation energy on surface properties and adhesion strength of TiN films deposited on aluminum by magnetron sputtering," *Mater. Sci. Eng. A*, **415**, 140–144 (2006).
20. W. C. Oliver and G. M. Pharr, "An improved technique for determining hardness and elastic modulus using load and displacement sensing indentation experiments," *J. Mater. Res.*, **7**, No. 6, 1564–1583 (1992).
21. G. M. Pharr, G. M. Oliver, and F. B. Brotzen, "On the generality of the relationship among contact stiffness, contact area, and elastic modulus during indentation," *J. Mater. Res.*, **7**, No. 3, 613–617 (1992).

Received 22. 11. 2013